GA–A26290

THE GENERAL ATOMICS FUSION THEORY PROGRAM REPORT FOR GRANT YEAR 2008

by
PROJECT STAFF

OCTOBER 2008

GENERAL ATOMICS

DISCLAIMER

GA–A26290

THE GENERAL ATOMICS FUSION THEORY PROGRAM REPORT FOR GRANT YEAR 2008

by
PROJECT STAFF

Work supported by
the U.S. Department of Energy
under Grant No. DE-FG03-95ER54309

GENERAL ATOMICS PROJECT 03726
OCTOBER 2008

ABSTRACT

The objective of the fusion theory program at General Atomics (GA) is to significantly advance our scientific understanding of the physics of fusion plasmas and to support the DIII-D and other tokamak experiments as well as ITER research activities. The program plan is aimed at contributing significantly to the Fusion Energy Science, the Tokamak Concept Improvement, and ITER goals of the Office of Fusion Energy Sciences (OFES). Significant progress was made in each of the important areas of our research program during the last grant year GY08. This includes development of a working model of the pedestal height EPED1 based on physics parameters that have been successfully shown to have the most impact on the pedestal height in DIII-D experiments, identification of low and high-n energetic-particle driven Toroidal Alfven Eigenmodes (TAEs) in gyro-kinetic calculations using the GYRO code, development and extensive testing of the new trapped gyro-Landau fluid (TGLF) transport model, performance of comprehensive numerical experiments using the GYRO code aimed at understanding the fundamental "zonal-flow/drift-wave paradigm," and development of a new gyro-kinetic neoclassical transport code NEO-GK and a new Integrated Modeling and Fitting tool IMFIT to support tokamak research and operation.

TABLE OF CONTENTS

1. HIGHLIGHTS OF THEORY WORK IN GY08

During the past grant year, significant progress was made in each of the important areas of our research program:

- Development of a working model of the pedestal height EPED1 based on physics parameters that have been successfully shown to have the most impact on the pedestal height in DIII-D experiments.
- Demonstration using the new kinetic MARS-F code that self-consistent inclusion of kinetic effect in RWM stability calculations modifies the eigenfunction and the kinetic stabilization effect is less than that deduced from perturbation treatment.
- Identification of low and high-n energetic-particle driven Toroidal Alfven Eigenmodes (TAEs) in gyro-kinetic calculations using the GYRO code that are most unstable within the expected Fu-Cheng Alfven frequency gap.
- Extensive testing of the TGLF transport model including validation of TGLF against a large database of tokamak discharges, a set of DIII-D ITER-demo discharges, and data from MAST and NSTX.
- Performance of comprehensive numerical experiments aimed at understanding the fundamental "zonal-flow/drift-wave paradigm" for nonlinear saturation of turbulent transport using GYRO with interesting results.
- Demonstration using the 3D MHD code NIMROD that the Rosenbluth runaway-electron criterion may be satisfied in an ITER equilibrium shut-down by massive D_2 dilution cooling due to inherent differences in the ITER operating regime from the DIII-D equilibrium previously studied.
- Demonstration using the new TGLF transport model that in a hybrid discharge a large fraction of electron transport can be driven by the high-k modes and that plasma transport increases substantially when going from infinite aspect-ratio shifted-circle geometry to shaped toroidal geometry (Miller model) due to increase in trapped-particle fraction.
- Development of a new gyro-kinetic neoclassical transport code NEO-GK that computes the neoclassical transport coefficients directly from solution of the distribution function based on a hierarchy of equations derived by expanding the drift-kinetic equation.
- Demonstration using the ideal MHD code GATO that the poloidal displacement may play an important role in the stability of the ideal quasi-interchange and internal kink modes in the sawtooth and the reconnection process.

- Demonstration using GYRO that the stabilization effects from $E \times B$ shear likely plays a role in overriding the sub-critical blow-up in DIII-D medium and very high β / β_{crit} discharges.
- Demonstration that fusion gains of over 20 may be achieved for solid-liner Magnetic Target Fusion (MTF) if high density FRC plasma can be formed and compressed.
- Development of an integrated modeling and fitting code IMFIT to support tokamak research and operation that is based on PYTHON and the Task Flow Architecture with extensive Graphical User Interfaces to ease management of various modeling tasks.
- Development of a 1D time-dependent fast current quench code FCQ to study the effect of various fueling sources on the current quench and runaway electron production and to explore the effects of "volumetric fueling" by liquid jets or a train of pellets.

As a consequence of these results, scientists from the Theory Group were selected to give a number of invited talks and colloquia as highlighted in the next section. Sections 3–6 provide more detailed descriptions of the advances and achievements made in each of the major areas.

2. SIGNIFICANT PRESENTATIONS IN GY08

2008 PRESENTATIONS

- 50th APS DPP meeting in Dallas, TX November 17-21, 2008:
  - E.A. Belli, invited presentation: "Drift-Kinetic Simulations of Neoclassical Transport."
  - P.B. Snyder, invited presentation: "Development and Validation of a Predictive Model for the Pedestal Height."
- 22nd IAEA Fusion Energy Conference in Geneva, Switzerland October 13-18, 2008:
  - C. Holland, oral presentation: "Validation of Gyrokinetic Transport Simulations Using DIII-D Core Turbulence Measurements."
  - V.A. Izzo, presentation: "RMP Enhancement Transport and Rotation Screening in DIII-D Simulations."
  - P.B. Snyder, presentation: "Pedestal Stability Comparison and ITER Pedestal Prediction."
  - G.M. Staebler, presentation: "Testing the Trapped Gyro-Landau Fluid Transport Model with Data from Tokamaks and Spherical Tori."
- 49th APS DPP meeting in Orlando, FL November 12-16, 2007:
  - J.E. Kinsey, invited presentation: "First Transport Code Simulations Using the TGLF Model."
  - V.A. Izzo, invited presentation: "MHD Simulations of Disruption Mitigation on DIII-D and Alcator C-Mod."
- International Sherwood Fusion Theory Conference in Boulder, CO March 31 through April 2, 2008:
  - E.A. Belli, invited presentation: "Drift-Kinetic Simulations of Neoclassical transport."
  - M.S. Chu, invited presentation: "Modeling of Resistive Wall Mode with Full Kinetic Damping."
- 21st US Transport Task Force Workshop in Boulder, CO March 25 - 28 2008:
  - J. Candy, presentation: "Progress on TGYRO: The Steady-State Gyrokinetic Transport Code."
  - M.S. Chu, oral presentation: "Modeling of Resistive Wall Mode with Full Kinetic Damping."

  - R.E. Waltz, presentation: "Numerical Experiments in the Drift-wave Zonal Flow Paradigm."
  - J.E. Kinsey, invited presentation: "Development and Validation of the Next Generation Trapped Gyro-Landau-Fluid Transport Model."
- Pedestal ITPA meeting in San Diego on April 30, 2008:
  - P.B. Snyder, presentation: "Developing and Testing a Predictive Model of the Pedestal Height (EPED1)."
- 4th US-PRC Magnetic Fusion Collaboration Workshop in Austin, Texas May 5-6, 2008:
  - V.S. Chan, presentation: "Overview of the DIII-D Five-Year Research Plan."
  - L.L. Lao, presentation: "Development of an Integrated Modeling Tool to Support DIII-D and EAST Research and Operation."
  - G. Li, presentation: "Integration of Equilibrium, MHD Stability, and Transport to Model DIII-D Pedestal Physics and ELMs."
  - Q. Ren, presentation: "Modeling of Momentum Transport in DIII-D Discharges with and without MHD Activities."
- 35th European Physical Society Conference on Plasma Physics in Hersonissos, Crete, Greece June 9-13, 2008:
  - R.E. Waltz, oral presentation: "Gyrokinetic Theory and Simulation of Angular Momentum Transport."
- US-Japan RF Workshop at PPPL February 27-28, 2008:
  - M. Choi, presentation: "The Coupling of 5D Particle Code with 2D Full-Wave Code for Plasma-Wave Interaction Simulation."
- SciDAC 2008 Conference in Seattle, WA July 13-17, 2008:
  - C. Holland, presentation: "Validating Simulations of Core Tokamak Turbulence: Current Status and Future Directions."
- SCcADS Workshop on Petascale Applications and Performance Strategies in Snowbird, UT July 14-17, 2008:
  - J. Candy, presentation: "TGYRO/TGLF/NEO."
- Opening Meeting for the International and Scientific Advisory Committees (CMFT) for the Center for Magnetic Fusion Theory, Chinese Academy of Science in Hefei, China September 2-3, 2008:
  - V.S. Chan, presentation: "Modeling Ion Cyclotron Heating Using Monte-Carlo Method."

  - M.S. Chu, presentation: "Modeling of Resistive Wall Mode with Full Kinetic Damping."
  - L.L. Lao, presentation: "Development of an Integrated Modeling Tool for Tokamak Research and Operation."

- 12th Workshop on MHD Stability Control at Columbia University, New York, NY November 18-20, 2007:
  - V.A. Izzo, presentation: "MHD Simulations of Disruption Mitigation on Alcator C-Mod and DIII-D, and Recent Experimental Highlights."
- Plasma Jet Workshop at LANL January 24-25, 2008:
  - P. Parks, invited presentation: "On the Efficacy of Imploding Plasma Liners for Magnetized Fusion Target Compression."

3. ADVANCES IN MHD EQUILIBRIUM AND STABILITY RESEARCH

3.1. EFIT EQUILIBRIUM RECONSTRUCTION USING SXR DATA

The method of using internal magnetic surface information from soft X-ray measurements to facilitate equilibrium reconstruction has been implemented and tested using EFIT. Reconstruction results show that the shape of the safety-factor q-profile in DIII-D can be generally determined from the information inferred from surfaces of constant soft X-ray emissivity. Magnetic surfaces and the q-profile reconstructed using external magnetic and SXR data agree reasonably with those using magnetic and Motional Stark Effect (MSE) data.

A study to investigate the effects of H-mode edge pedestal on the divertor shaping coil current requirement using EFIT was completed, as part of the ITER STAC support activities. The results show that as edge current increases and internal inductance ℓ_i decreases, more divertor coil current is required to maintain the plasma shape, as expected.

3.2. EDGE STABILITY AND PEDESTAL MODEL DEVELOPMENT

A new predictive model of the pedestal height, EPED1, has been developed and tested, with encouraging results. The pressure at the top of the edge transport barrier, or "pedestal height" has a large impact on core confinement and overall fusion performance, and its prediction is an important element of performance projection and optimization in ITER. Calculations of peeling-ballooning stability of the pedestal using the ELITE code, give a constraint on the maximum pedestal height as a function of the width. Combining a simple model of the pedestal width $\Delta_{PED} \propto \sqrt{\beta_P^{PED}}$ with direct peeling-ballooning stability calculations using ELITE yields a new predictive model for the pedestal height and width, called EPED1. EPED1 was used to make and present pedestal height predictions before a dedicated pedestal experiment on DIII-D in March 2008. In the experiment, triangularity, current and magnetic field were varied, resulting in a variation of more than an order of magnitude in pedestal height. The EPED1 predictions showed very good agreement with the observations across the full range (Fig. 1). Predicted to measured ratios of 1.03±0.13 in height and 0.93±0.15 in width are found over 17 discharges in which pedestal height varied a factor of 10 and width a factor of 3. EPED1 has also been used to predict the pedestal height and width in a set of DIII-D ITER demonstration discharges. The ratio of predicted/observed height in these four cases is 1.00±0.14.

The pedestal stability of a set of hydrogen discharges in the ITER shape has also been studied in detail. Full stability analysis of measured equilibria for five such discharges finds that the pedestal is constrained, and ELMs triggered by, peeling-ballooning modes, just as in standard deuterium discharges. Predictions with the EPED1 model also find reasonable agreement with the observed pedestal height and width, suggesting that there is no (or very

weak) ion mass dependence in the pedestal width. This would appear to support the $\Delta_{PED} \propto \sqrt{\beta_P^{PED}}$ width model used in EPED1.

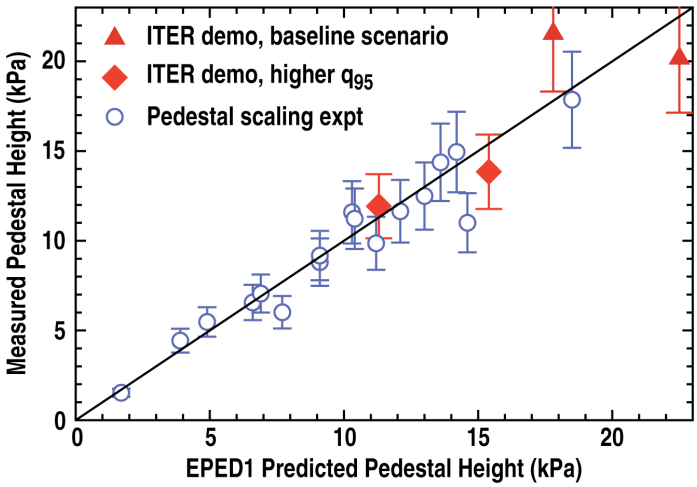

Fig. 1. A new predictive model of the pedestal height, EPED1, was used to make pedestal height predictions before a DIII-D experiment on March 4, 2008. Full analysis of these 17 discharges is now completed. Comparison between EPED1 predicted and observed pedestal height in this experiment is shown in blue circles, with an overall ratio of predicted to observed pedestal height of 1.03±0.13. EPED1 predictions have also been made for 4 DIII-D ITER demonstration discharges (red symbols) with good agreement found.

Edge stability analysis using ELITE has also been conducted on the first discharges showing clear evidence of quiescent H-mode (QH-mode) in the absence of counter-injected neutral beams. Analysis results show that these co-injected QH-mode discharges exist in the same kink/peeling constrained part of parameter space as traditional counter QH-modes, with rotation shear profiles similar to counter-injected QH-modes (but with opposite sign), as expected from our previously proposed QH-mode model (Snyder 2007).

3.3. RWM STABILITY WITH FULL KINETIC DAMPING

A full drift-kinetic version of MARS-F based on the kinetic formulation of MHD response has been developed. The kinetic integrals are evaluated in a general toroidal geometry with flow, and self-consistently incorporated into the MHD formulation. The energy and momentum fluxes across the plasma surface are expressed in terms of the MHD perturbations. The new kinetic MARS-F has been exercised to show that self-consistent inclusion of the kinetic effect in RWM calculations modifies the eigenfunction and the kinetic stabilization effect is less than that deduced from the perturbation treatment.

3.4. TAE MODE IDENTIFICATIONS USING GYRO

High-n energetic-particle driven Toroidal Alfven Eigenmodes (TAEs) were identified in gyro-kinetic calculations using the GYRO code. The modes are driven by energetic particles

with velocity equal to Alfven velocity ($k_Y \rho_s$ = 0.001–0.050) and are most unstable within the expected Fu-Cheng Alfven frequency gap. This is illustrated in Fig. 2. These linear modes were obtained in a small cyclic flux tube with only one singular surface. However, a large cyclic flux tube stretching across the whole plasma gives similar growth rates. Replacing the cyclic with zero boundary conditions will lower the growth rates. Future work will study these modes using DIII-D experimental profiles and compare with MHD-hybrid codes like NOVA-K.

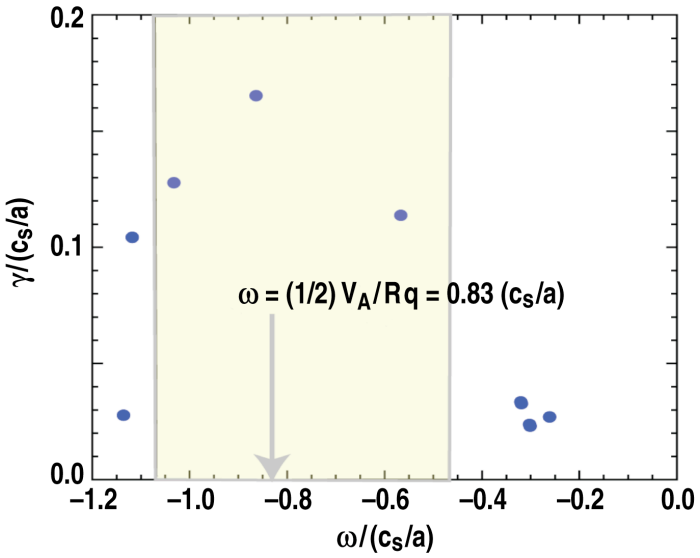

Fig. 2. Normalized TAE mode growth rates computed using GYRO showing that the modes are most unstable within the expected Fu-Chang gap.

Low-n global eigenmode instabilities in equilibria with full shaped magnetic geometry reconstructed from experimental measurements in DIII-D have also been demonstrated using the GYRO code. These instabilities were driven by an assumed density gradient profile of energetic particles (with the background plasma gradients reset to zero). The characteristics of the frequency and growth rates are similar to those from local high-n flux tubes simulations in GYRO.

3.5. NIMROD SIMULATIONS AND DEVELOPMENT

3.5.1. NIMROD 2/1 NTM Simulations

NIMROD simulations have been carried out to compare with high-resolution fast-framing camera images of a 2/1 NTM in DIII-D. The simulations begin with an EFIT reconstruction obtained in the presence of the saturated NTM (thus including the modified bootstrap current in the equilibrium, though it is not evolved self-consistently in NIMROD). The simulations is initialized with 2/1 seed island of ~ 4 cm at the outboard mid-plane. The island grows for ~ 8 ms and saturates at a width of ~ 10 cm at the outboard mid-plane

(Fig. 3), qualitatively consistent with experimental observations. A synthetic diagnostic will be developed in conjunction with M. Van Zeeland (who made the DIII-D measurements) to directly compare the visible bremsstrahlung emission between simulation and experiment.

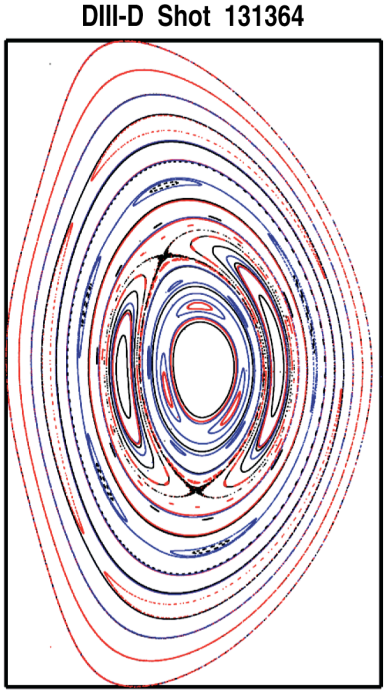

Fig. 3. Projection of magnetic field lines into a toroidal plane for a NIMROD simulation of a 2/1 NTM in DIII-D. The island grows for ~ 8 ms and saturates at a width ~ 10 cm qualitatively consistent with experimental observations.

3.5.2. NIMROD RMP Rotational Screening

The Fitzpatrick theory of plasma response to applied resonant magnetic perturbations (RMP) includes both an amplification of resonant modes, and a rotation screening effect. A non-rotating RMP simulation of DIII-D with NIMROD is used to numerically determine the amplification term alone. Then the theoretical rotational screening factors for two rotating simulations are combined with the non-rotating amplification factors to predict the total mode amplitude in the rotating simulations, in order to test just the screening portion of the theory against NIMROD results. The predicted $n = 3$ mode amplitude as a function of m has a very similar m dependence to the NIMROD results, but the overall mode amplitudes tend to be significantly higher in the simulations. The most likely explanation for this failure of the theory is that it does not include toroidal mode coupling effects. This will be tested by repeating the NIMROD simulations in a periodic linear geometry, which should adhere more closely to the theory. However, the results point to the importance of toroidal effects which are ignored in some RMP calculations that sacrifice realistic geometry in order to achieve higher Lundquist number.

3.5.3. NIMROD Dilution-Cooling Disruption Simulations

NIMROD has also been used to simulate a disruption mitigation scenario in which the deuterium density of the plasma is increased 100 fold by some method (pellet train or liquid jet) that allows penetration of the impurities to the core. A 1% in situ carbon fraction is assumed, which produces strong radiation in the plasma cooled by dilution, particularly at the edge. A radiation-induced cold front propagates from the edge to the core. The induced pressure gradients, which determine the stability during the cold-front propagation, are set by a Pfirsch-Schlüter ion heat transport model, which produces large perpendicular transport at these densities. As a result, the plasma remains MHD stable until the cooling wave approaches the center, at which point a 1/1 MHD event acts to rapidly reduce the core temperature and current density. Just prior to the 1/1 event, the central current density is nearly three times its initial value, which produces strong electric fields at the dilution reduced plasma temperatures, transiently exceeding the Rosenbluth criterion for runaway avalanching. Further evaluations of runaway electron production and avalanching (which the 100 fold density increase is designed to prevent) are required for this scenario. Comparisons between the 3D simulations and a 1D code incorporating a 1/1 Kadomtsev mixing model will be performed.

NIMROD simulations have also been extended to ITER plasma. Because the simulation begins following a ~150 fold dilution and corresponding cooling of the plasma, the ITER simulation can be run at realistic resistivity to produce predictions of the thermal and current quench time scales without the need for rescaling. The Rosenbluth ratio that determines runaway electron avalanche amplification can be tracked throughout the plasma shutdown. Unlike DIII-D simulations, ITER plasmas are found to remain below the Rosenbluth criteria (in the amplification-free regime), due to inherent differences in the ITER operating regime. These results and DIII-D simulations are being compared with the 1D dilution cooling simulations of Parks and Wu. More detailed runaway electron post-processing analysis has been developed to track acceleration and confinement of high-energy electrons.

The coupling of the KPRAD atomic physics code with NIMROD, which is used to perform disruption mitigation simulations, has been incorporated into the release version of NIMROD. This will keep the KPRAD version up to date with other NIMROD code developments and make it available to other users. Successful verification tests of disruption mitigation cases have been performed to test the new NIMROD version against the previous NIMROD/KPRAD code.

3.6. GATO IDEAL SAWTOOTH STABILITY ANALYSIS

A detailed analysis of the ideal quasi-interchange and internal kink modes and their roles in the sawtooth and the reconnection process revealed that the crucial difference between them is the poloidal displacement. When analyzing only the radial displacement, the previous results from the comparison of the ideal stability calculations from the bean and oval cross

section were mixed and ambiguous. In the new analysis, preliminary indications show that the oval is unstable to the ideal quasi-interchange over most of the sawtooth cycle and that the bean undergoes an internal kink at the time of the sawtooth crash. This is consistent with the observation of a distinct reconnection event for the bean shape discharge and no clear reconnection event for the oval case.

3.7. EHO STABILITY STUDY

The stability property of the EHO mode in DIII-D QH-mode discharges has been studied. A few instabilities have been found. The plasma could be weakly unstable to an ideal $n = 1$ mode, or it could be unstable to a resistive $n = 1$ mode. However, so far, all of the modes found show the effect of rotation stabilization. This mode has an unconventional rotation dependence in that it is destabilized by rotation.

4. ADVANCES IN TRANSPORT RESEARCH

4.1. GYRO APPLICATIONS

4.1.1. GYRO Numerical Experiments

GYRO has been used for numerical experiments aimed at understanding the fundamental "zonal-flow/drift-wave paradigm" for nonlinear saturation of turbulent transport and in particular, difference, if any, between nonlinear saturation via zero mean frequency zonal flows and via GAMs which tend to dominate the high-q edge. The main practical conclusion from the simulation numerical experiments is that the drift wave fluctuation (potential) intensity (at each mode wave number) should scale roughly like the product of the GAM frequency and the linear growth rate rather than the square of the linear growth rate, as often assumed. The latter is physically inconsistent in that it is well understood that drift wave turbulence is nonlinearly stabilized by the radial modes (zonal flows and GAMs), whereas the square of the linear growth rate makes no reference to the radial mode physics. The GLF23 and TGLF saturation models are roughly consistent with the new result, but MMM95 is not.

A second project of GYRO numerical experiments was started to properly test the quasi-linear approximation that is a crucial ingredient for building transport models. All physically comprehensive models like MMM95, GLF23, and TGLF rely on it. The transport flow is a spectral sum product of the quasi-linear weight and the fluctuation (potential) intensity (at each mode in the spectrum). In these models, the quasi-linear weight is computed from the linear dispersion relation (or simulation) and the fluctuation intensity is from a model. In the GYRO test of the quasi-linear approximation, there is a *two-step* method: first a linear simulation to get the quasi-linear weight, then a second nonlinear simulation to get the actual nonlinear fluctuation intensity (at each mode).

The product of the quasi-linear weight and the actual nonlinear fluctuation intensity provide the true quasi-linear transport that is then compared with the actual nonlinear transport. We find that in many (if not all) cases the quasi-linear transport *in each channel* is about C_{ql} = 1.4–1.8 times the actual nonlinear transport. *Quasi-linear transport is a practical success when the overage factor C_{ql} is exactly the same in each channel.* We can look at the mode spectrum of the overage factor C_{ql} to find that the higher k modes have the greatest overage. Fortunately the higher k modes always make a smaller contribution to transport unless the lower k modes are $E \times B$ shear stabilized. Failure may be because the test method does not include subdominant modes, whereas quasi-linear transport models (like GLF23 and TGLF) do include subdominant modes.

To include subdominant modes we are looking at a *one-step* test: GYRO is run with ion and electron plasma species at full density and ion and electron tracer species at vanishing

densities having no feedback on the potential fluctuations (four species). If the plasma and tracer species have exactly the same gyrokinetic dynamical equation, then tracer and plasma diffusivities are identical as expected. If the tracer species has the nonlinear interaction deleted, tracer diffusivity is then a quasi-linear diffusivity (with the true nonlinear potential spectrum) and the plasma diffusivities remain the true diffusivities. Again we see the average overage is 1.4–1.8. Various ideas to modify the quasi-linear weight so as to bring down the overage factor or make them more nearly equal across channels have been tried without success. The obvious idea to add a $k^2 D$ damping to linear modes did not help for any choice of D. The quasi-linear theory seems to work best for the energy channel (i.e., $\chi_e^{QL}/\chi_i^{QL} \sim \chi_e^{NL}/\chi_i^{NL}$) and sometimes poorly for the particle channels (i.e., $D_e^{QL}/\chi_i^{QL} \neq D_e^{NL}/\chi_i^{NL}$). Strangely quasi-linear theory works fairly well for the (kinetic electron) GA-std case ($a/L_T = 3,\ a/L_n = 1$) as well as the GA-TEM1 ($a/L_T = 2,\ a/L_n = 2$), and GA-TEM2 ($a/L_T = 1,\ a/L_n = 3$), but not so well when the gradients move far away (e.g., for GA-std with $a/L_{T_e} = 3$ but $a/L_{T_1} >> 3$).

4.1.2. GYRO Simulations at Very High β and the Sub-Critical β Mystery

Since the first GYRO β scan for transport (Cyclone 2005), we have not been able to get a saturated (finite) transport state with β/β_{crit} greater than about one-half. The GENE code agrees well with GYRO for $\beta/\beta_{crit} \leq 1/2$ but also cannot get above this sub-critical value. The transport decreases to rather small levels just before the sub-critical value is reached. Numerous repeat GYRO simulations of this scan have been done with larger numerical simulation boxes and higher grid resolution, and also at other parameters. The sub-critical point remains and the key ingredients have not yet been identified. Magnetic flutter transport relative to $E \times B$ transport increases with β/β_{crit} but there is no evidence that the sub-critical blow-up is associated with magnetic flutter. It is generally believed that the critical point is not associated with a subdominant mode like the KBM. The current best hypothesis is that it is associated with the onset of magnetic island overlap stochasticity, but that has not been verified. A medium high beta shot $\beta/\beta_{crit} \sim 1/2$ and another very high beta $\beta/\beta_{crit} \sim 1$ shot from DIII-D have been simulated with GYRO to understand why the sub-critical effect has not been seen in real experiments like DIII-D. It appears from these preliminary runs that the DIII-D $E \times B$ shear stabilization can override the sub-critical blow-up. If the $E \times B$ shear is removed, the blow-up returns.

4.2. TGLF TRANSPORT MODEL DEVELOPMENT AND TESTING

The saturation rule for TGLF was extended to include an impurity ion species. The weightings of the intensity for different ion species were determined by comparing to GYRO simulations with helium and carbon. The results suggest that the ion charge density fraction provides the best weight. It was expected that the fractional contribution to Z_{eff} would have been a better choice. The kinetic impurity results were also compared with simple dilution. For carbon simple dilution was found to be a good approximation as long as the impurity

density gradient length is not too different from the main ion density gradient length. Simple dilution is a poor approximation when the charge density fraction exceeds 50%.

Work to improve the collision model in TGLF was continued. A breakthrough in the construction of the electron-ion collision model for TGLF was made. It was discovered that the large collision frequency limit of the trapped-particle distribution function should be the distribution function without trapped particles. Previously it was thought that the trapped particle distribution function was driven to either zero or an adiabatic response. A new form of the model using this limit gives a much better fit to the kinetic numerical solution. This new model agrees very well with GYRO particle and electron energy fluxes improving over the APS07 version of the collisions model. The new model however reduces the ion energy flux too much compared to GYRO. The GYRO ion energy flux is half way between the new model and the APS07 model. The new model predicts somewhat higher temperatures for the tokamak database. The predicted fusion power for ITER was almost doubled using the new collision model indicating the sensitivity of the prediction to collisions. It appears that the numerical kinetic solution is introducing an artificial damping due to truncation error of the Legendre polynomial expansion. This may be why the low collision frequency ion energy fluxes do not yet agree with the GYRO results. Unfortunately, adding more Legendre polynomials is not possible due to numerical problems with the matrix inversion. A boundary layer approach to the trapped-passing boundary is showing promise in overcoming this difficulty.

A first validation of the TGLF transport model against a large database of tokamak discharges was completed. Compared to its predecessor GLF23, TGLF has much better fidelity to gyro-kinetic linear stability and non-linear turbulence driven fluxes computed with the GYRO code. Both GLF23 and TGLF are quasi-linear models, but the improved physics of TGLF result in better agreement between predicted and measured temperature and density profiles. One of the surprising results was how large the predicted high-k electron transport was compared to the low-k level. This is illustrated in Fig. 4 for a DIII-D L-mode and a DIII-D hybrid discharge. For the L-mode discharge, the high-k modes were contributing ~30% to χ_e at $\rho = 0.6$. For the hybrid discharge, the high-k modes were predicted to produce ~90% to χ_e in the same region.

A test of the TGLF transport model with data from MAST has been completed in collaboration with Greg Colyer of Culham Laboratory. It was found that outside the sawtooth region ($q > 1$) TGLF predicted the ion and electron temperatures to within 17% and 26% respectively for eight discharges. The electron temperature prediction was on average 11% too high whereas the ion temperature was 4% too low. It was found that electron-ion collisions play an important role in improving the transport by reducing the trapped electron drive. The new electron-ion collision model in TGLF, which improves the fidelity to gyro-kinetic theory, also resulted in an improved prediction of the MAST temperatures. In addition, the shaped geometry modification to the Chang-Hinton formula proposed by Belli

and Candy to give better agreement with the NEO code numerical neoclassical ion thermal diffusivity has a significant impact on the ion temperature prediction. The Belli-Candy modification yields much better agreement with the data. This motivates coupling the NEO code to the transport code in the future.

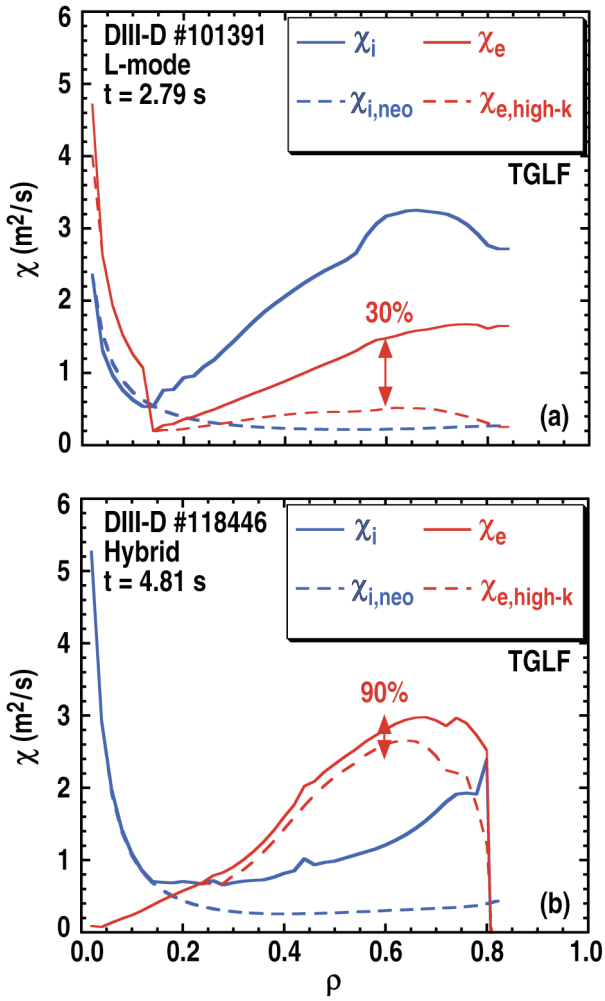

Fig. 4. TGLF predicted energy diffusivities for (a) DIII-D L-mode discharge #101391 and (b) DIII-D hybrid discharge #118446.

In collaboration with Ed Doyle from UCLA, a set of DIII-D ITER demo discharges has been analyzed using the TGLF transport model. These discharges were carried out in an effort to evaluate the leading scenarios for ITER operation including the baseline or conventional H-mode, hybrid, advanced inductive, and steady-state scenarios. These discharges incorporated key elements of the ITER scenarios including the plasma shape, aspect ratio and the value of I/aB. The target values of β_N and H_{98} were also replicated in DIII-D. Therefore, it is of interest to validate the TGLF model using this dataset in order to improve our confidence in predicting the performance of ITER. Using the XPTOR transport code, it was found that the RMS errors in the profiles for the four scenarios is comparable to

the RMS errors found previously in benchmarking the model against a database of conventional DIII-D H-mode discharges. The overall average RMS errors for the ITER demo discharges was 10% and 16% for T_i and T_e compared to 15% and 8% obtained for the conventional H-mode dataset (Fig. 5).

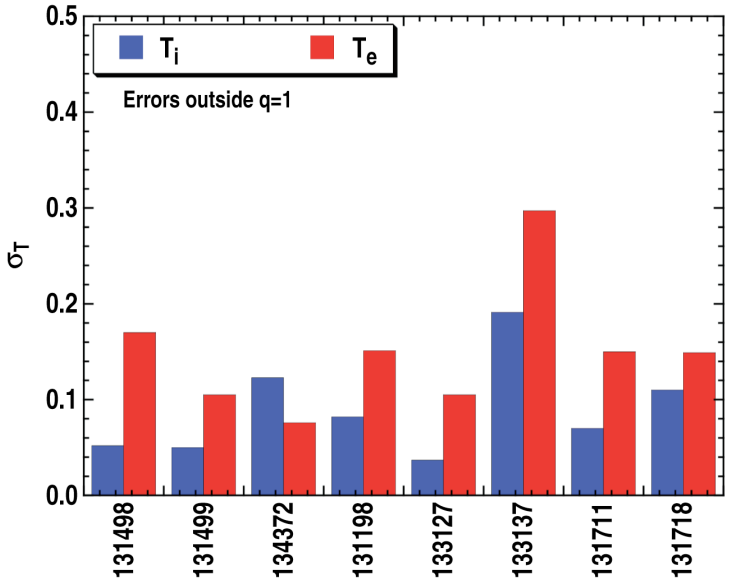

Fig. 5. RMS errors in the predicted ion (blue) and electron (red) temperature profiles using the TGLF model for eight DIII-D ITER demo discharges.

4.3. STEADY-STATE GYROKINETIC TRANSPORT CODE DEVELOPMENT AND TESTING

A new overlay code TGYRO was set up to call GYRO as a subroutine. TGYRO has a "local" and "global" option. The global TGYRO uses the 2004 feedback method to locally adjust the temperature and density gradients until the local simulated radial transport flows match the input experimental flows. When the feedback iterations come to steady state, the gradients are radial integrated from a "pivot radius" (say $\rho = 0.6$) to give the "transport solution" temperature and density profiles. Hopefully these transported profiles are within the error bars of the experimental profiles from which the process starts. The problem is to find the proper feedback strength to get to the steady state efficiently. We have been quite successful in doing large slice ($\rho = 0.3$–0.8) "full physics" DIII-D L-mode transport solutions within say 2000–3000 GYRO time units (compared to the usual 500 time units for a fixed gradient GYRO simulation). DIII-D H-modes operate very close to the threshold and convergence has been proven to be quite difficult. Since the transport levels are quite low in H-modes, we have also added a computation of Chang-Hinton ion neoclassical energy flow to GYRO. Neoclassical transport cannot be ignored when the $E \times B$ shear stabilizes so much of the low-k transport. We have recently realized from TGLF transport work that high-k ETG electron transport may be as much as 50% (90%) of H-mode electron transport.

The TGYRO gyrokinetic transport solver now has the ability to call the TGLF model, in addition to GYRO to compute particle and energy fluxes. This flexibility will be used to speed up local TGYRO calculations near threshold and in other situations where the GYRO fluxes are too expensive to be practical. New benchmarks with XPTOR (with Miller geometry) show close agreement for a particular DIII-D benchmark case. The iteration stability is being improved when using fluxes from gyrokinetic simulations. An iteration scheme that uses TGLF to compute the Newton direction (i.e., the Jacobian) even for fully gyrokinetic transport simulations will be explored. A simple interface to TGLF has also been written. Although this was needed for use with TGYRO, it simplifies calling to TGLF in general.

4.4. NEOCLASSICAL TRANSPORT DEVELOPMENT AND TESTING

Work on the development and testing of the new gyro-kinetic neoclassical transport code NEO-GK was continued. NEO-GK is a δf Eulerian code and is based on a hierarchy of equations derived by expanding the drift-kinetic equation in powers of the ratio of the ion gyro-radius to the system size. Unlike NCLASS, NEO-GK computes the neoclassical transport coefficients directly from solution of the distribution function. NEO-GK extends previous numerical studies by including the self-consistent coupling of electrons and multiple ion species and the calculation of the first-order electrostatic potential via coupling with the Poisson equation. Fully general geometry is included, using either a full numerical equilibrium or the Miller local parameterized equilibrium model. Three model collision operators have been implemented (the full Hirshman-Sigmar operator, the reduced Hirshman-Sigmar operator, and the Connor model).

NEO-GK has also been upgraded to include the effects of strong toroidal rotation on neoclassical transport, thus eliminating the diamagnetic ordering limit and completing the description of the second-order transport. The code has been successfully benchmarked with the Hinton and Wong analytic theory for a pure plasma. For studies of impure rotating plasmas, a general enhancement of the magnitude of the ion and impurity particle and energy fluxes is found, as expected due to the increase in the effective fraction of trapped particles as a result of the non-uniform poloidal redistribution due to the centrifugal force. While an increase in the poloidal flows is also found, even with strong rotation the effect is too weak to explain the large impurity flows observed in DIII-D experiments. A journal paper describing the numerical methods used in NEO-GK and highlighting the new results is in progress.

5. ADVANCES IN RF HEATING AND FUELING RESEARCH

5.1. ORBIT-RF/AORSA COUPLING AND BENCHMARK

To simulate the resonant interaction of ICRF waves with tokamak plasma, the 2D full wave code AORSA has been coupled to the ORBIT-RF code. Since AORSA represents wave electric fields as a sum of multiple wave modes in a cylindrical coordinate, we applied the space-time averaging technique to the AORSA wave fields, which is verified by formally deriving the electromagnetic quasi-linear diffusion term from the Vlasov equation with the assumption of random phase approximation. A 2D mapping program was rewritten to map AORSA wave electric fields in cylindrical coordinate to the Boozer coordinate used in ORBIT-RF. Then, the mapped AORSA wave fields were spatially averaged over the rapid variation in poloidal flux coordinate. Comparative calculations of the local power damping of ICRF wave using ORBIT-RF/AORSA and AORSA/CQL3D for C-Mod hydrogen minority ICRF heating were carried out.

Extensive benchmarking activity between ORBIT-RF and AORSA is also being carried out to model the fundamental to high harmonic ICRF wave heating in the Alcator C-Mod and DIII-D tokamaks. The 2D linear full wave code, AORSA, assumes zero orbit width and constant wave–particle interaction time, while the 5D Monte-Carlo Hamiltonian ion guiding center code, ORBIT-RF, includes finite orbit effect and a more accurate treatment of the wave-particle interaction time. Reference cases are simplified. Either resonant thermal minority or fast beam ions are assumed as Maxwellian distribution with tails on axis. A single toroidal wavenumber is used. Perpendicular wave spectrum is calculated from a cold plasma dispersion relation. Linear heating models are being benchmarked using two different numerical approaches: ORBIT-RF with Monte-Carlo particle and AORSA with linear full wave. Local power absorption, calculated from ORBIT-RF without updating resonant ions characteristics, is compared with AORSA calculated power absorption. The two codes show excellent agreement in modeling of fundamental ICRF wave heating of Maxwellian plasma in the Alcator C-Mod tokamak, while a factor of two difference has been found in modeling of high harmonic ICRF heating cases in the DIII-D tokamak towards the plasma edge. To understand these differences, orbit losses will be examined and perpendicular wave spectrum, modeled in these simulations from a cold plasma dispersion relation, will be more accurately simulated to include hot plasma effects.

5.2. DISRUPTION MITIGATION MODELING

A 1D time-dependent fast current quench FCQ code to study the effect of various fueling sources on the current quench and runaway electron production has been developed. The model includes a thermal energy balance equation with radiation and heat transport. We also applied FCQ to explore the effects of “volumetric fueling” by liquid jets or a train of pellets.

As previously reported, significant current rearrangement occurs when the balance state is approached. Specifically, the balance state is thermally unstable when radiation cooling is only balanced against ohmic heating. The natural tendency for the current density to diffuse from cooler regions into hotter regions promotes the instability by removing the Ohmic heating source from the originally cooler region. This reinforces cooling and hastens more current diffusion. The large current density gradients may excite current driven MHD instabilities. It turns out, fortunately, that a substantial amount of the original thermal plasma energy is dissipated by radiation before the current density peaks form. We found that inclusion of thermal diffusion is necessary to inhibit current density peaking on or near the magnetic axis that helps to prevent the $m = 1$ instability, as q_0 drops below unity. To address the $m = 1$ kink instability, the Kadomtsev magnetic reconnection model has been implemented into the FCQ code to address the issue of the on-axis safety factor q_0 dropping below unity and the associated $n = 1$, $m = 1$ kink instability. Both the Pfirsch-Schlüter energy diffusion term and the Kadomtsev modules have been extensively tested. The reconnection is found to effectively prevent current lock-up near the magnetic axis, and to promote faster plasma current decay.

Preliminary modeling of the ablation of a polystyrene (PS) shell predicts that a 500 m/s pellet containing densely packed dust grains easily crosses the $q = 2$ surface in DIII-D before complete ablation. Encapsulation of dust grains by PS shell pellets is being considered for delivering massive density increase to the plasma for the purpose of mitigating disruptions. Surface ablation proceeds by pyrolysis (thermal decomposition) of PS, which favors the production of its styrene monomer, C8H8. The sacrificial shell undergoes ablation while in flight through the hot plasma and shielding the interior dust grains from the plasma heat flux until the shell fully ablates. Once that happens, the bare “dust ball” is expected to undergo fragmentation and entrapment inside a radiatively cooled plasma, thereby allowing massive plasma densification. Experiments injecting small 2 mm hollow shell pellets, filled with argon gas by permeation, are being planned on DIII-D in order to compare the shell burnout distance with model predictions. With increasing temperature in the downstream ablation flow, the monomer gas decomposes into smaller molecules, free radicals, and ions. This “cracking” process will be included in future gas dynamic modeling, as it represents a significant heat sink in the ablation flow field, and tends to lower the pellet mass loss rate.

6. ADVANCES IN INTEGRATED MODELING AND INNOVATIVE CONFINEMENT RESEARCH

6.1. IMFIT AND ONETWO DEVELOPMENT

A version of the integrated modeling and fitting code IMFIT based on PYTHON and the Task Flow Architecture was developed. The design consists of a framework and six component controllers that manage various equilibrium, transport, and stability tasks using Fortran codes such as EFIT, TOQ, ONETWO, ELITE and GATO. The development of the framework and the six component controllers is nearly completed. Work to integrate the component controllers under the framework and the development of the Graphical User Interfaces (GUI's) for various Physics Managers is in progress.

A version of the TGLF confinement model is installed and operational in the GCNMP code. Access to this model for ONETWO and PTRANSP is based on a client-server protocol that allows us to retain a single CVS based repository for GCNMP to serve both transport codes and functioning in a serial or parallel mode, independent of the transport driver. However, it is not feasible to run the TGLF model in single processor mode and much of the recent work is based on developing parallel models that will decrease the running time and maintain compatibility with PTRANSP and ONETWO. The parallel models used in GCNMP (master/slave and domain decomposition) are now developed as far as we can take them without introducing major intrusions into the TGLF module itself. Thus, further refinement will require close collaboration with the original developers of the TGLF module. Due to the large number of refinements introduced into GCNMP as a consequence of including the TGLF model, it is particularly important to validate the new methods. This validation is currently underway using DIII-D ITER-demo discharges for which extensive XPTOR results are available.

6.2. MAGNETIZED TARGET FUSION (MTF) USING PLASMA JETS

During GY08, most of our activity converged on intense opposition to the start of a large-scale DOE-funded jet experiment under consideration at LLNL, using an array of plasma jets to form a spherical plasma liner. This motivated us to prepare for the MTF pre-HEDLP meeting and the following HEDLP subpanel meeting on August 25, in an effort to promote and deepen our technical arguments. Our objection is grounded on the recently published Physics of Plasma paper by Parks. Although we did not attend the pre-HEDLP MTF meeting, our work and this paper was discussed a fair amount at the meeting, and was generally thought to be correct, although detailed interpretation of the numerical examples offered was challenged by Francis Thio. It was unanimously recognized that the paper showed clearly that achieving the needed plasma liner momentum density on target to get significant stagnation pressure is difficult with plasma jets, mainly because of their low mass density.

Still, many of the MTF committee members felt that fundamentally, at least, the idea that converging supersonic liner flows can achieve substantial pressure multiplication over initial ram pressure of the liner is of general interest and worth investigation.

Our strategy involves a two-pronged approach. First, we have submitted a proposal with Roman Samulyak at Stony Brook University to HEDLP. We proposed to perform 1D, 2D and 3D simulations of converging supersonic plasma jets, forming the plasma liner, and study the corresponding oblique shock problem. We will study the implosion of the plasma liner on the magnetized plasma target by resolving Rayleigh-Taylor instabilities in 2D and 3D, and estimate the efficiency of the method. We will also explore a new idea of using dusty plasmas for efficiency improvement. Simulations will be thoroughly compared with simpler 1D calculations and those using alternative methods such as the smoothed particle hydrodynamics, and experimental data (if available). The 1D study has already been started with another collaborator Volodymyr Makhin (formerly UNR) using the MHRDR code. The results showed that the idealized Parks' scaling law $A \cong C^2$ describing the liner ram pressure amplification A due to liner radial convergence C, is valid *only* when C is small, less than 30 or so. Increasing C further causes a deviation of A below the ideal curve; eventually, A saturates with increasing C. We also did FLUENT simulation of *individual* supersonic ($M >> 1$) plasma jets on their way to the "merging surface" (before jet merging to form a plasma liner). A set of supersonic jet configurations are simulated, covering M = 10, 20, 30, and 60, and 1 μs and 2 μs pulse times. Results indicate that the divergence of the gas jet is remarkable under low M numbers, e.g., 10 and 20. This set of simulation suggests further reassessment of the concept, since the density and ram pressure of the jet may be seriously degraded after traveling only a meter, and several meters of travel will be needed in a reactor scenario.

Secondly, alongside our plasma liner MTF efforts we constructed a new model of magnetized target decompression with heavy metal (incompressible) liner/tamper. New fusion gain calculations for solid liner MTF indicate gains of over 20 can be achieved if high density $\sim 2 \times 10^{18}$ cm^{-3} FRC plasma can be formed and compressed. These gains are vey attractive and far superior to the essentially "epsilon" gains possible for Plasma Jet MTF. Our work was presented by Dr. Glen Wurden at the HEDLP subcommittee meeting on August 25 and was well received by MTF researchers, because it dispelled the gain ~ 1 "urban myth" that some members of the ICF community have about the potential of solid liner MTF.

7. PUBLICATIONS

PRIMARY THEORY AUTHORS FOR 2008

E.A. Belli and J. Candy, "Kinetic Calculation of Neoclassical Transport including Self-Consistent Electron and Impurity Dynamics," Plasmas Phys. Control. Fusion **50**, 095010 (2008).

E.A. Belli and J. Candy, "An Eulerian Method for Solution of the Multispecies Drift-Kinetic Equation," submitted to Plasmas Phys. Control. Fusion.

S. Braun, P. Helander, E.A. Belli, and J. Candy, "Effects of Impurities on Collisional Zonal-Flow Damping in Tokamaks," submitted to Phys. Plasmas.

M. Choi, A.D. Turnbull, V.S. Chan, M.S. Chu, L.L. Lao, Y.M. Jeon, G. Li, Q. Ren, R.I. Pinsker, "Sawtooth Control using Fast Wave-Accelerated Beam Ions in the DIII-D Tokamak ," Phys. Plasmas **14**, 112517 (2007).

V.A. Izzo, D.G. Whyte, R.S. Granetz, P.B. Parks, E.M. Hollmann, L.L. Lao, J.C. Wesley, "MHD Simulations of Massive Gas Injection into Alcator C-Mod and DIII-D Plasmas," Phys. Plasmas **15**, 056109 (2008).

V.A. Izzo and I. Joseph, "RMP Enhanced Transport and Rotational Screening in Simulations of DIII-D Plasmas," Phys. Plasmas **48**, 115004 (2008).

J.E. Kinsey, R.E. Waltz, J. Candy, "The Effect of Plasma Shaping on Turbulent Transport and E×B Shear Quenching in Nonlinear Gyrokinetic Simulations," Phys. Plasmas **14**, 102306 (2007).

J.E. Kinsey, G.M. Staebler, and R.E. Waltz, J. Candy, "The First Transport Code Simulations Using the TGLF Model," Phys. Plasmas **15**, 055908 (2008).

G. Li, S.J. Wang, L.L. Lao, A.D. Turnbull, M.S. Chu, D.P. Brennan, R.J. Groebner, L. Zhao, "Ideal MHD Stability of Double Transport Barrier Plasmas in DIII-D," Nucl. Fusion **48**, 015001 (2008).

Y.Q. Liu, M.S. Chu, C.G. Gimblett, and R.J. Hastie "Magnetic Drift Kinetic Damping of the Resistive Wall Mode in Large Aspect Ratio Tokamaks," Phys. Plasmas **15**, 092505 (2008).

P. Parks, "On the Efficacy of Imploding Plasma Liners for Magnetized Fusion Target Compression," Phys. Plasmas **15**, 062506 (2008).

J.P. Qian, L.L. Lao, Q.L. Ren, F. Volpe, H. Rinderknecht, and B.N. Wan. "Equilibrium Reconstruction of Plasma Profiles Based on Soft X-Ray Imaging in DIII-D," submitted to Nucl. Fusion.

R.E. Waltz, G.M. Staebler, J. Candy, and F. Hinton, "Gyrokinetic Theory and Simulation of Toroidal Angular Momentum," Phys. Plasmas **14**, 122507 (2007).

R.E. Waltz and G.M. Staebler, "Gyrokinetic Theory and Simulation of Turbulent Energy Exchange," Phys. Plasmas **15**, 014505 (2008).

R.E. Waltz and C. Holland, "Numerical Experiments on the Drift Wave - Zonal Flow Paradigm for Nonlinear Saturation," submitted to Phys. Plasmas.

S.K. Wong, V.S. Chan, and W.M. Solomon, "Poloidal Velocity of Impurity Ions in Neoclassical Theory," Phys. Plasmas **15**, 082503 (2008).

ACKNOWLEDGMENT

This work supported by the U.S. Department of Energy under Grant No. DE-FG03-95ER54309.